Available online at www.sciencedirect.com
SCIENCE DIRECT®
ELSEVIER
Journal of Nuclear Materials 319 (2003) 131–141
journal of nuclear materials
www.elsevier.com/locate/jnucmat

Modelling the behaviour of oxide fuels containing minor actinides with urania, thoria and zirconia matrices in an accelerator-driven system

V. Sobolev *, S. Lemehov, N. Messaoudi, P. Van Uffelen, H. Aït Abderrahim

Belgian Nuclear Research Centre, SCK • CEN, Boeretang 200, B-2400 Mol, Belgium

Abstract

The Belgian Nuclear Research Centre, SCK • CEN, is currently working on the pre-design of the multipurpose accelerator-driven system (ADS) MYRRHA. A demonstration of the possibility of transmutation of minor actinides and long-lived fission products with a realistic design of experimental fuel targets and prognosis of their behaviour under typical ADS conditions is an important task in the MYRRHA project. In the present article, the irradiation behaviour of three different oxide fuel mixtures, containing americium and plutonium – $(Am,Pu,U)O_{2-x}$ with urania matrix, $(Am,Pu,Th)O_{2-x}$ with thoria matrix and $(Am,Y,Pu,Zr)O_{2-x}$ with inert zirconia matrix stabilised by yttria – were simulated with the new fuel performance code MACROS, which is under development and testing at the SCK • CEN. All the fuel rods were considered to be of the same design and sizes: annular fuel pellets, helium bounded with the stainless steel cladding, and a large gas plenum. The liquid lead–bismuth eutectic was used as coolant. Typical irradiation conditions of the hottest fuel assembly of the MYRRHA subcritical core were pre-calculated with the MCNPX code and used in the following calculations as the input data. The results of prediction of the thermo-mechanical behaviour of the designed rods with the considered fuels during three irradiation cycles of 90 EFPD are presented and discussed.

1. Introduction

The high level radioactive waste (HLW), produced by nuclear power plants, presents one of the most important problems of this century. Different approaches are proposed for a long-term management of HLW. The transmutation of transuranium elements (TRU) and long-lived fission products (LLFP) in critical and subcritical nuclear reactors is considered to be a very promising solution [1]. During the last years the interest continued to grow to using the accelerator-driven subcritical systems (ADS) for the TRU incineration, firstly plutonium (Pu) and minor actinides (MA), and for the LLFP transmutation. The first step to the development of a prototype ADS-transmuter is the design of a small experimental ADS. The Belgian Nuclear Research Centre, SCK • CEN is developing such ADS named MYRRHA (multipurpose hybrid research reactor for high-tech applications) [2].

The choice of a subcritical core strongly impacts performances of the ADS. On one hand, a fast neutron spectrum is needed to fission efficiently MA (Np, Am, Cm), because their 'fission-to-capture' cross-sections ratio is larger at high neutron energies [3]. On the other hand, significantly higher neutron absorption cross-sections of nuclides at the thermal spectrum allow to transmute easier LLFP (^{129}I, ^{99}Tc) and also make effective the double-step transmutation of MA, where in the first step a MA nuclide is transformed into a fissile isotope by capture of a thermal or epithermal neutron, and then this isotope is split by another thermal neutron in

* Corresponding author. Tel.: +32-14 33 22 67; fax: +32-14 32 15 29.
E-mail address: vsobolev@sckcen.be (V. Sobolev).

0022-3115/03/$ - see front matter © 2003 Elsevier Science B.V. All rights reserved.
doi:10.1016/S0022-3115(03)00145-4

the second step [4]. In order to study the both possibilities, an experimental ADS has to be capable to provide neutrons at least with two types of spectrum: fast and thermal.

Two strategies of the MA transmutation are now under consideration in order to reach a high discharge burnup at a low burnup reactivity loss after one cycle of the core operation. The first one uses a low power density and requires a high inventory of MA; in the second, a high power density and a larger number of irradiation cycles are needed [5]. The second strategy is more suitable for the experimental ADS MYRRHA. Although it requires a more frequent refuelling, the more convenient experimental conditions can be assured in this case. Moreover, the fuel life-time in the fast cores is often limited by radiation damage of the fuel pin cladding.

Development of the thermo-mechanical fuel performance code MACROS (multipurpose advanced code for research and development of oxide fuel systems) is a step made by the SCK • CEN in modelling of the thermo-mechanical behaviour of fuel rods with actinide–oxide mixtures [6]. The MACROS code has been created on the basis of the extended version of the PLUTON code [7] in combination with the fuel performance code ASFAD [8]. The database of the material properties was modified to include new oxide fuels and mixtures, cladding materials and coolants of interest.

Three different oxide fuels containing americium and plutonium – $(Am,Pu,U)O_{2-x}$ with urania matrix, $(Am,Pu,Th)O_{2-x}$ with thoria matrix and $(Am,Y,Pu,Zr)O_{2-x}$ with the inert yttrium stabilised zirconia matrix (APZ) – were selected for this study. The fuel rods considered to be of the same design and sizes: annular pellets, helium bounded with the stainless steel cladding and a large gas plenum. The liquid lead–bismuth eutectic is used as coolant. Typical irradiation conditions of the hottest fuel assembly of the MYRRHA subcritical core were pre-calculated with the MCNPX code [9] and used in the following calculations as input data. The preliminary modelling of evolution of the fuel isotopic composition was performed with the ORIGEN 2.1 code [10]. The obtained results were used to validate the neutronic module of the MACROS code. Then modelling of the thermo-mechanical behaviour of the fuel rods was performed. This paper discusses the preliminary results obtained in modelling of the quasi-steady-state behaviour of three target-fuel rods with $Am_{0.25}Pu_{0.25}U_{0.5}O_2$, $Am_{0.25}Pu_{0.25}Th_{0.5}O_{2-x}$, $Am_{0.25}Y_{0.1}Pu_{0.25}Zr_{0.4}O_{2-x}$ fuel (designated in this article as APU, APT and APZ respectively) in the MYRRHA subcritical core during three cycles of irradiation (each of 90 EFPD) with maintenance periods of 30 d.

The paper is organised as follows. Section 2 gives a brief presentation of the MYRRHA ADS and describes the irradiation conditions in the hottest assembly. The fuel composition and main parameters of the studied fuel rods are provided in Section 3. A general description of the fuel performance code MACROS is given in Section 4. Section 5 discusses the main results of the modelling.

2. ADS MYRRHA

SCK • CEN is currently working on the pre-design of a multipurpose ADS MYRRHA devoted to research and development. The MYRRHA ADS concept was selected after a preliminary screening of different candidate concepts, aiming at large research capabilities for the TRU and LLFP transmutation, tests of new fuel, reactor material studies and medical applications [2].

The preliminary design of both, the subcritical core pins and the experimental fuel-target rods with MA or LLFP, is an important task in the MYRRHA project. To meet the aimed research goals and to assure a large experimental flexibility, four different neutron spectrum zones – thermal, resonant, fast and quasi-spallation – were foreseen in the current core design. The basic fast spectrum zone is composed of hexagonal fuel assemblies of fuel pins with $(Pu,U)O_2$ MOX containing 20–30 wt% of the reactor-grade plutonium in heavy metal (HM). This zone is very suitable for the reactor material irradiation and for the MA transmutation studies. The thermal spectrum zone represents an inserted in-pile section at the core periphery, which is named in the relevant technical documents 'thermal island' (Fig. 1). This thermal island will enable the transmutation experiments with LLFP and MA, the irradiation experiments with LWR fuels and the production of radioisotopes.

Whereas $(Pu,U)O_2$ MOX fuel is expected to be used as driver fuel in the subcritical core at the first stage of the MYRRHA operation, the different sorts of experimental fuel rods containing TRU and LLFP will be tested in the experimental channels disposed nearby the spallation target, in the fast core, in the thermal island and in the reflector. At the next stage, a part of the driver fuel in the core can be replaced with the fuel containing TRU.

Maximising the fast neutron flux and minimising the core power at the fixed neutron multiplication factor of $k_{\text{eff}} \sim 0.95$ were chosen as the primary performance objectives in the MYRRHA core design. After neutron modelling and optimisation of some design parameters the total thermal power level of about 40 MW and the fast neutron flux of $\sim 10^{15}$ $\text{cm}^{-2}\,\text{s}^{-1}$ (peak value) were obtained in pre-design calculations.

3. Preliminary design of a fuel-target pin

Three oxide mixtures containing $(Am,Pu)O_2$ fuel and different matrices were selected for modelling: urania

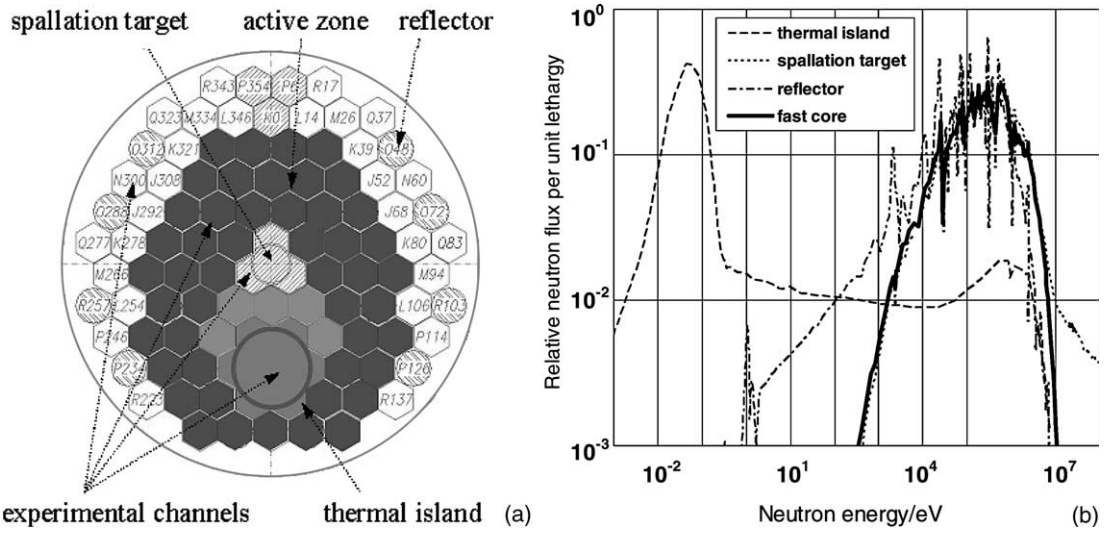

Fig. 1. Typical core configuration with 'thermal island' (a) and neuron spectra in different experimental channels (b) of the MYRRHA ADS.

based $(Am,Pu,U)O_{2-x}$, thoria based $(Am,Pu,Th)O_{2-x}$ and inert matrix based $(Am,Y,Pu,Zr)O_{2-x}$. The first fuel is expected to be more close to $(Pu,U)O_2$ and was selected as an intermediate case between the driver MOX and two non-uranium fuels. Using thoria matrix in the TRU–oxide mixture fuels has a potential to improve the fuel performance, due to a high melting point and a thermal conductivity of thoria. A smaller reactivity swing with increasing burnup may be expected for cores with this fuel due to conversion of ^{232}Th in ^{233}U. The disadvantages of thoria are a slightly higher fission gas yield per fission, and a more difficult reprocessing [11,12]. The third fuel, with the yttrium stabilised zirconia (YSZ) matrix, is considered last years as one of the most promising candidates for MA burning [13,14]. The zirconia and thoria based fuels are also studied as candidates for the MA incineration in the ADS-transmuter in the project FUTURE (the EURATOM 5th Framework Programme [15]). The first neutronic estimates showed that rather realistic figures for the ADS-transmuter cores could be obtained with these fuels when 'Pu-to-Am' ratio is between 0.7 and 1.0, and at least a half of the compound is matrix [16]. Following these recommendation, at the first stage of studies it was postulated that the studied fuels contain americium–plutonium oxide fuel mixture ($Am_{0.5}Pu_{0.5}O_2$) and matrix (UO_2, ThO_2 or YSZ) in equal quantities. Isotopic composition of Pu and Am has been taken from [5], where it was given for the retreated spent fuel discharged from a PWR assembly with average burnup of 33 MW d kg^{-1} after 10 years of its cooling. A depleted uranium was used in the fuel with urania matrix. Thorium in the thoria based fuel contains only one isotope ^{232}Th, as well as yttrium (^{89}Y) in the YSZ-based fuel. The natural isotopic composition was used for zirconium and oxygen [17]. Isotopic vectors of the elements are presented in Table 1.

All oxides of interest were assumed to be of MO_2 type and to have the face-centred cubic crystal structure. The oxide mixtures were considered as quasi-ideal solutions, and their lattice parameters, heat capacities and melting temperatures were calculated by using the Vegard's law. Thermal conductivity and other parameters were estimated with the models of the code MACROS

Table 1
The initial isotopic composition of elements in the experimental fuels [5,17]

U	Content (wt%)	Pu	Content (wt%)	Am	Content (wt%)	Zr	Content (wt%)
^{234}U	0.003	^{238}Pu	1.27	^{241}Am	84.503	^{90}Zr	50.71
^{235}U	0.404	^{239}Pu	61.88	^{242m}Am	0.247	^{91}Zr	11.18
^{236}U	0.010	^{240}Pu	23.50	^{243}Am	15.25	^{92}Zr	17.28
^{238}U	99.583	^{241}Pu	8.95			^{94}Zr	17.89
		^{242}Pu	4.40			^{96}Zr	2.94

Table 2
Some parameters of the studied fuels [11–14,17]

Fuel rod code	APU	APT	APZ
Fuel type	$Am_{0.5}Pu_{0.5}O_2$	$Am_{0.5}Pu_{0.5}O_2$	$Pu_{0.5}Am_{0.5}O_2$
Matrix type	UO_2	ThO_2	$Y_yZr_{1-y}O_{2-y/2}$
Fuel vs matrix fraction/mol	1:1	1:1	1:1
Molar mass ($g\,mol^{-1}$)	271.2	268.2	197.6
Theoretical density ($g\,cm^{-3}$)	10.71	10.75	8.65

(see the next chapter). The fuel codification used in the following sections below is given in Table 2. All the compounds were considered to be of 95% theoretical density (TD).

The choice and optimisation of the fuel cell composition and of the fuel pin is one of the key problems in the ADS-transmuter design. Some contradictory requirements should be satisfied: maximising the burnup rate, minimising the burnup reactivity loss, maximising the heat removal capabilities, maximising the space for experiments. Two most important requirements in the fuel pin design are fuel non-melting and non-damage of the cladding by inner or outer pressures and loads during the total fuel life [18]. Given the maximum desired power density in the core, the first criterion determines the pellet dimensions. The second criterion determines the clad diameter and thickness. At this stage we decided not to analyse different fuel geometries and to limit our studies only by a very widespread variant of a fuel rod with annular pellets helium bounded with the stainless steel cladding through a large gap.

The peak power density in the MYRRHA core with the $(Pu,U)O_2$ MOX (30 wt% Pu in HM) is about 1.3 $kW\,cm^{-3}$ [2]. The MA fuels under consideration contain 25 mol% of PuO_2 and 25 mol% of AmO_2. Neutronic estimates performed with ORIGEN 2.1 code [10] showed that the peak power density for the considered fuels is $\sim$1.4 $kW\,cm^{-3}$ under the same irradiation conditions. This value is rather close to that mentioned above and is within the limits of the MYRRHA fuel cooling capabilities.

In many well-known designs of the fuel rods for LMFBR (and also in the driver fuel pins of the MYRRHA ADS), a ratio of the pellet hole diameter to the pellet external diameter is 0.2–0.3 [19]. Taking into account a lower thermal conductivity of americium containing fuels [20], the value close to 0.3 has been chosen for this ratio, that allows about 30% reduction of the fuel maximum temperature in comparison with the solid pellet variant [19]. The lowest melting temperature and thermal conductivity among the considered oxides has $(Am,Pu)O_2$. An estimate based on the Vegard's law and on the recommendations given in [20–22] yields for this oxide $T_{melt} \sim 2500$–2600 K. Based on the mentioned above values and keeping some conservatism, the fuel

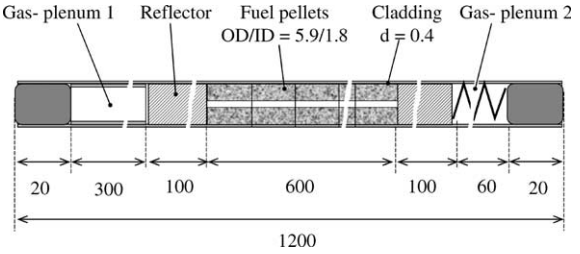

Fig. 2. Preliminary design of a fuel-target rod (sizes are given in mm).

pellets with the outer diameter of 5.9 mm and the hole of 1.8 mm have been chosen for the following analysis. The low-swelling martensitic stainless steel T91 [23] has been taken as the cladding material, which has good mechanic parameters and corrosion resistance in the liquid lead–bismuth environment [24]. The clad diameter of 6.9 mm and thickness of 0.4 mm was chosen, taking into accounting for the initial thermal expansion, corrosion and assuming that expected fuel swelling should be compensated during the irradiation period of 270 EFPD. The preliminary axial sizes of the fuel-target pins were postulated to be the same as those of the reference fuel rod of the MYRRHA subcritical core. Fig. 2 gives the schematics of the fuel rod design.

Having fixed the fuel pin geometry, we started with a more detailed modelling of the fuels behaviour by means of the MACROS code [6]. Behaviour of the three fuels mentioned above have been analysed at the typical MYRRHA operation conditions, when the total neutron flux in the positions of the fuel targets was kept constant.

4. MACROS fuel performance code

4.1. Origin of the MACROS code

The development of the thermo-mechanical fuel performance code MACROS at the SCK•CEN was mainly initiated by fuel research related to the MYRRHA ADS [2] and to the prototype ADS-burner. This code has been created on the basis of the fuel perfor-

mance code ASFAD [8] and the burnup code PLUTON [7]. The last has been originally developed as a supplementary neutronic code for the FEMAXI-V fuel performance code [25]. The database of the material properties was modified to include new oxide fuels, their mixtures and cladding materials. New geometry, neutronic and thermo-hydraulic modules were developed and lead–bismuth eutectic as coolant-moderator was introduced to simulate in-pile conditions of ADS with fast neutron subcritical cores. In view of an important role that helium may play during a long-term irradiation or storage of fuels, the burnup model of the original PLUTON code has also been modified to include the production of helium due to decay of α-emitters. This allowed accounting for both, thermo-mechanical and neutronic, effects at extended burnup simultaneously. So, the MACROS code is able to analyse the thermo-mechanical behaviour of a single fuel rod as well as to predict the evolution of the isotopic composition in fuel under typical ADS conditions.

4.2. Models

In the actinide stoichiometric dioxides of type MO_2 there are four atoms in an elementary cell. Thus, there will be three acoustic and nine optic modes of vibration. The acoustic modes were described with the Debye model and the optic modes with the one frequency Einstein model [26]. Moreover, the effect of thermal dilatation and the Schottky contribution were taken into account in a similar manner as it was proposed by Serizawa and Arai [27].

Linear thermal expansion coefficients of the components of oxide mixtures were calculated with the polynomial temperature dependencies of the lattice parameter recommended by Yamashita et al. [28]. Where it was not possible, the thermodynamic relationship bounding the volumetric thermal expansion coefficient and the isobaric specific heat capacity was used [27].

Thermal conductivity has a strong impact on fuel performance. Unfortunately, very limited data exist on thermal conductivity of the actinide oxides (except UO_2) and their mixtures. Two major heat transport mechanisms were included in the model of the MACROS code: the lattice and charge carriers' conductions. The Debye–Callaway approach to modelling the lattice thermal conductivity [29] was used. The model for the lattice thermal conductivity of actinide fuels developed based on this approach was already presented in [30,31]. Taking into account that contribution of the charge carriers (electrons) is relatively small in the considered temperature range, it was estimated with Widemann–Frantz law [32] (where needed). In view of our general interest in modelling of actinide oxide fuels, the following resistive imperfections were taken into account: phonons, isolated point defects (e.g., vacancies, interstitials, chemical impurities and isotopes), line imperfections (typically for in-pile conditions this is track network caused by fission fragments), intra-granular gas bubbles. The thermal conductivity correlations for pure thoria, urania, plutonia, americia and zirconia and for $(Pu,U)O_2$ MOX were first developed and verified with the data found in open literature (references are reported in [30,31]), then they were applied for calculation of thermal conductivities of $(Am,Pu,U)O_{2-x}$, $(Am,Pu,Th)O_{2-x}$ and $(Am,Pu,Zr,Y)O_{2-x}$ fuels.

In view of the important role that helium, produced by TRU-decay, may play during a long-term irradiation or storage of the considered fuels, the PLUTON burnup model, which is a part of MACROS code neutronic module, has been extended to include the production of helium due to actinide emitters. Indeed, it is well-known that a significant amount of helium is generated with time in the fuels with a high content of minor actinides [33]. The presence of plutonium and americium in the fuel leads to build-up of americium and curium isotopes. The most important actinide emitters of helium are ^{238}Pu, ^{241}Am, ^{242}Am, ^{242}Cm, ^{243}Cm and ^{244}Cm. Other transuranium isotopes may contribute to the helium production indirectly via transmutation. A rather complete scheme is described in the joint CEA/ITU technical note [34]. This scheme was used in the extended PLUTON model. The model for release of fission and decay gases has been updated taking into account the developments made at the SCK • CEN [35]. Some new results have recently been communicated by Damen et al. [36], Wiss et al. [37], van Veen [38] and Scharm et al. [39] on helium release. However, a more detailed analysis is needed before their implementation in the models. This work is still under way.

5. Results of modelling

5.1. Irradiation history and evolution of the fuel composition

Preliminary estimations of evolution of the isotopic composition and heating rates in the peak pellets of the considered fuels, as well as of the production of xenon, krypton and helium, were first performed with the ORIGEN 2.1 code [10]. Calculations were made under conditions of the constant neutron flux in the hottest fuel assembly of the MYRRHA core. The cross-sections used in the code libraries were weighted by the neutron spectrum. The results of these calculations for the APT peak pellet are presented in Fig. 3 as functions of time for three cycles of irradiation (one cycle is 90 EFPD) followed by maintenance periods of 30 d. The MA and Pu burnouts after each cycle, related to the initial contents of Am and Pu respectively, are given for the three fuels in Table 3.

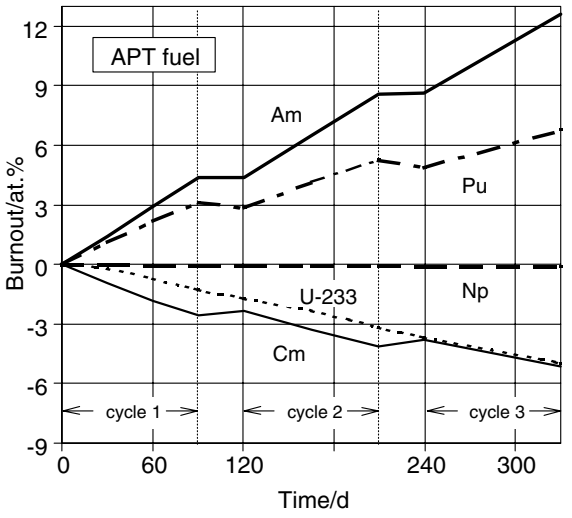

Fig. 3. Burnout (+) and production (−) of minor actinides (Np, Am, Cm) and plutonium (Pu) related to the initial content of americium and plutonium respectively in the APT rod: $(Am_{0.25}Pu_{0.25}Th_{0.5})O_{2-x}$.

From Table 3 one can see that relative rates of MA incineration under considered conditions are very similar for all three compounds and reach about 7.3–7.4 at.% after the third cycle. As a matter of fact the americium burnout reaches 12.6% in all three samples, but at the same time 5.13 at.% of curium (related to the initial americium content) is produced. It is evident that non-uranium fuels (APT and APZ samples in Table 2) have higher rates of Pu burning: ~6.8 at.% comparing to 2.44 at.% in the APU sample where the conversion of U into Pu takes place. In the sample with thoria matrix (APT), ^{233}U was produced in quantity of about 5 at.% of the initial Pu content. This situation is very close to a partial equilibrium when burned plutonium is replaced by ^{233}U (see Fig. 3). At certain extent, this effect can be considered as positive which can help to keep the reactivity level in the subcritical core of the ADS-transmuter without large compensating reserve of the accelerator.

It should be mentioned that values presented in Table 3 were obtained for homogeneous fuels. In heterogeneous ones, where $(Am,Pu)O_2$ is usually concentrated in the micro-particles of 50–100 μm in diameter uniformly distributed in the matrice, the burning rates would be slightly lower because of differences in self-shielding effect. It is interesting to note that the content of curium decreases and that of plutonium increases during the maintenance periods between the irradiation cycles (Fig. 3). This is mainly explained by α-decay of ^{242}Cm and ^{244}Cm, which generate ^{238}Pu and ^{240}Pu respectively. Degradation of the plutonium quality due to this effect is illustrated in Table 4 where the Pu-vector before and after irradiation is presented.

The amount of helium produced in the fuels increases very rapidly with time (Fig. 4). Because the greatest part of helium is produced by α-decay of curium and americium, its content continues to increase also during the reactor stops. At the end of irradiation period its concentration can reach 0.3–0.4 at.%.

The time dependence of the liner heat-generation rate (LHGR) in the peak pellets of the studied fuel rods is illustrated by Fig. 5. One can see that during all three operation cycles the LHGR values are very close: 360–380 $W\,cm^{-1}$. The lowest LHGR has the APT rod with thoria matrix. In all rods, LHGR shows a tendency to a slow decrease with operation time, mainly due to burning of Pu. After three operation cycles this reduction in IMF rod (APZ) is about 7%. Reproduction of fissile isotopes (^{239}Pu in urania and ^{233}U in thoria) makes this decrease lower in APU and APT rods: 2.6% and ~0.4% respectively. Just after every stop, the residual power is about 5% of the initial level, but reduces for ~10 times by the end of the first stop and for ~7 times by the end of the second.

5.2. Fuel temperatures, swelling and gap evolution

The power densities and irradiation histories, obtained with the ORIGEN code, were used as inputs for the fuel performance code MACROS to model thermomechanical behaviour of the stadied fuel rods. Evolution

Table 3
Burnout and build-up of TRU in the considered fuels

	Burnout (at.%)								
	1st cycle			2nd cycle			3rd cycle		
	APU	APT	APZ	APU	APT	APZ	APU	APT	APZ
MA total	1.72	1.76	1.78	4.29	4.36	4.38	7.29	7.37	7.41
Am	4.38	4.36	4.38	8.58	8.68	8.59	12.6	12.6	12.6
Cm	−2.57	−2.56	−2.56	−4.15	−4.15	−4.15	−5.13	−5.13	−5.13
Np	−0.10	−0.03	−0.03	−0.15	−0.07	−0.07	−0.19	−0.11	−0.11
Pu	1.58	3.12	3.12	2.25	5.26	5.26	2.44	6.79	6.82
$^{233}U + ^{235}U$	0.052	−1.29	$<-10^{-3}$	0.102	−3.20	$<-10^{-3}$	0.15	−4.97	$<-10^{-3}$

Table 4
Change of the plutonium isotopic vector in the APZ fuel

Pu-isotope	Relative fraction (wt%)	
	At start	After 3 cycles
^{238}Pu	1.27	4.65
^{239}Pu	61.88	55.11
^{240}Pu	23.50	25.85
^{241}Pu	8.95	8.09
^{242}Pu	4.40	6.30

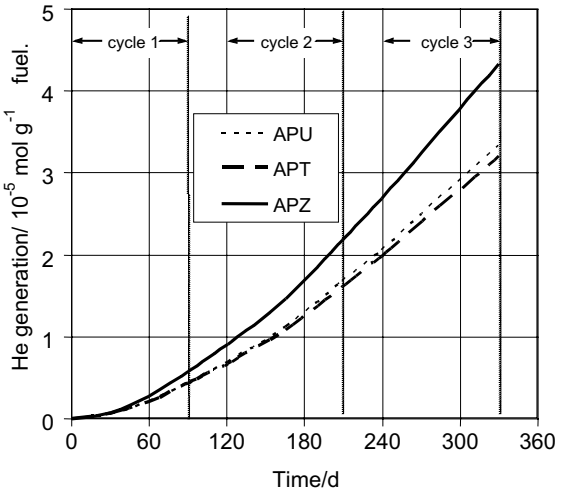

Fig. 4. Helium generation in the studied fuels during three cycles of irradiation: APU = $(Am_{0.25}Pu_{0.25}U_{0.5})O_{2-x}$; APT = $(Am_{0.25}Pu_{0.25}Th_{0.5})O_{2-x}$; APZ = $(Am_{0.25}Y_{0.1}Pu_{0.25}Zr_{0.4})O_{2-x}$.

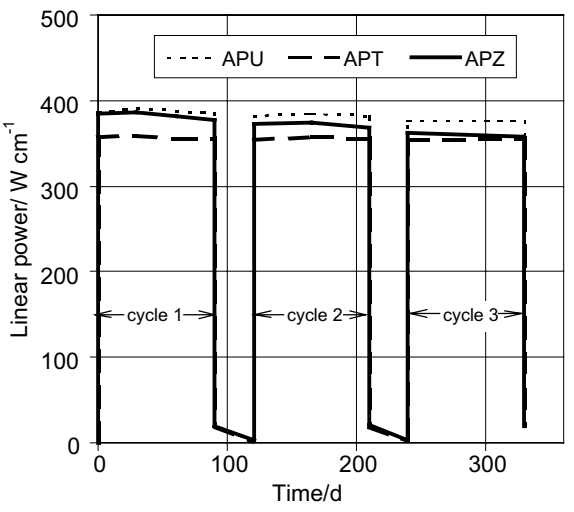

Fig. 5. Linear power density evolution in the studied fuels during three cycles of irradiation: APU = $(Am_{0.25}Pu_{0.25}U_{0.5})O_{2-x}$: APT = $(Am_{0.25}Pu_{0.25}Th_{0.5})O_{2-x}$; APZ = $(Am_{0.25}Y_{0.1}Pu_{0.25}Zr_{0.4})O_{2-x}$.

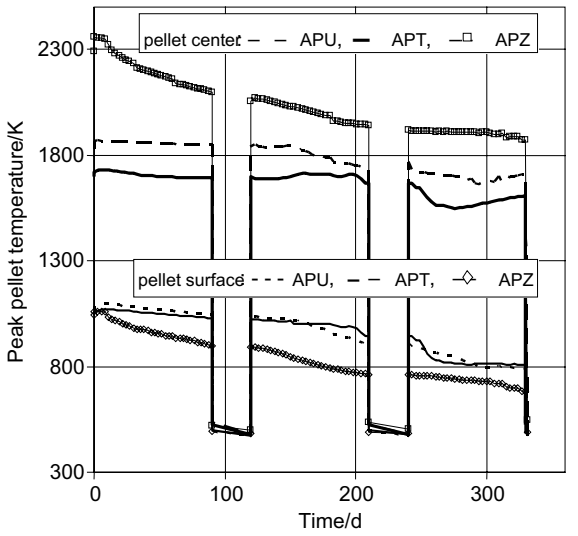

Fig. 6. Evolution of the central and surface temperatures of the peak pellets: APU = $(Am_{0.25}Pu_{0.25}U_{0.5})O_{2-x}$; APT = $(Am_{0.25}Pu_{0.25}Th_{0.5})O_{2-x}$; APZ = $(Am_{0.25}Y_{0.1}Pu_{0.25}Zr_{0.4})O_{2-x}$.

of the central and surface temperatures of the peak pellets with time is presented in Fig. 6.

Two major phenomena are important for temperature calculations: in-pile fuel thermal conductivity and actual shape of the radial power profile. The new model for thermal conductivity of the fuels of interest [6] was used in the MACROS code to treat the first of them. In order to model the power radial profile in the fuel pellets, a one-cell multienergy group approach (originally developed for the PLUTON burnup model [7]) has been used. The spectrum of the incoming neutrons has been taken as a boundary condition to find the thermal neutron flux depression (minor effects in the ADS core) and the attenuation of epithermal neutron flux. It was also assumed that ADS fuels are transparent for the fast neutrons with energy $\geqslant$1 MeV. The multigroup equations described in [6] then have been used to compute the radial distributions of fertile and fissile isotopes, the group macroscopic absorption and fission cross-sections and the resulting attenuation of neutron flux in the fuels towards the centre. Finally, the radial power profiles, which turn to be quite non-uniform for all types of considered ADS fuels, were determined.

The levels of the maximum fuel temperatures are rather high (1600–2400 K). The highest central temperature and temperature difference across the pellet radius has the APZ sample. This is mainly due to the lowest thermal conductivity of the YSZ matrix. The radial temperature difference across the APZ pellets remains about constant during the whole operation period, indicating that irradiation defects give only a small contribution to the initial fuel thermal resistance. A monotonic decrease of its central temperature with

irradiation is related to the decreasing of the pellet surface temperature, which is caused by a reduction of the pellet-cladding gap. In two other samples (APT and APU) the decrease of the pellet central temperature is lower, because the effect of the gap closing is partially compensated by an increase in the radial temperature difference caused by the irradiation induced degradation of thermal conductivity. The lowest central temperature has APT sample, due to a slightly lower LHGR and a higher thermal conductivity. The fuel central temperature in the APU sample is between these two extreme cases.

The pellet surface temperatures are very similar for APU and APT samples during the whole irradiation period and decrease gradually with irradiation time (Fig. 6). This behaviour is explained by the fact that thermal expansion coefficients are close for the considered materials and by the large design gap between the fuel pellets and cladding (200 μm diametric). The lower fuel surface temperatures were obtained for APZ sample due to a lower pellet-cladding gap. This is a result of higher thermal extension and swelling (Fig. 7(a)).

The rate of fuel swelling is correlated with the mean temperature level – the highest swelling is observed for the APZ sample, the medium for APU and the lowest for APT. The irradiation induced densification of fuel at the beginning of the first cycle, demonstrated by negative values in Fig. 7(a), is compensated by swelling very rapidly in the APZ fuel, and in the second half of the first cycle in APT and APU. Roughly, the swelling rate during the operation period follows the temperature evolution.

The evolution of the diametric pellet-cladding gap in the studied samples is illustrated in Fig. 7(b). After an abrupt reduction (from 200 to about 110–120 μm), caused by the fuel thermal expansion and by pellets cracking during the reactor start up, followed by a slight increase related to densification, the gaps decrease monotonically during irradiation due to the fuel swelling. The 'cold' gap values are given between the cycles. The pellet-cladding gaps remain still open in all rods after 270 EFPD. However, in the APZ rod it is close to zero by the end of the third cycle.

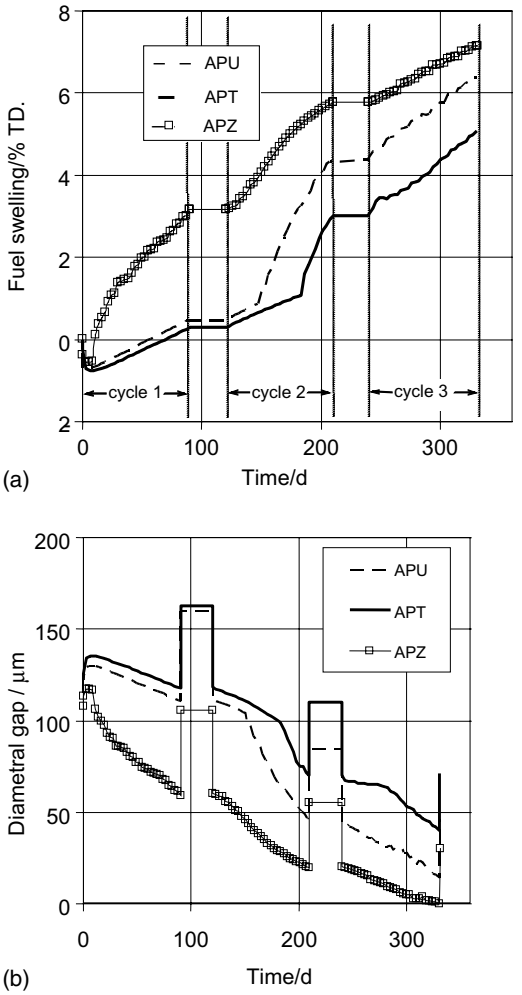

Fig. 7. Fuel swelling (a) and the 'pellet-clading' gap evolution in the studied fuels: APU = $(Am_{0.25}Pu_{0.25}U_{0.5})O_{2-x}$; APT = $(Am_{0.25}Pu_{0.25}Th_{0.5})O_{2-x}$; APZ = $(Am_{0.25}Y_{0.1}Pu_{0.25}Zr_{0.4})O_{2-x}$.

5.3. Fission and decay gas production and release

The amount of helium produced in fuels containing americium is very important. One hour after the ADS start the helium fraction is already about 8% of the summary yield of the noble gas atoms (Xe, Kr, He) in fuel; at the end of the third cycle, it is more than 50% (Fig. 8). The relative rates of helium production in the APU, APT and APZ fuels are different but very close. The maximum amount is produced in IMF fuel (APZ). The evolution of amounts of He, Kr and Xe produced in the peak pellet of this rod is shown in Fig. 9.

At the beginning of the reactor operation, the generated helium, krypton and xenon diffuse and are captured by the intra-granular and inter-granular traps (grain boundaries, nanometric-bubbles and pores), which are not saturated yet. They increase the internal pellet stress, which, in its turn, causes swelling.

The effective release of Xe and Kr from APU and APT fuels starts in the first half of the second cycle. The beginning of their release from APZ fuel is delayed by about 60 d due to higher saturation capacities of traps in YSZ matrix. During the third cycle the release of Xe and Kr continues with increasing rates in all samples. At the end of irradiation about 20% of the produced xenon and krypton is released in the APU and APT peak pellets and about 13% in APZ (Fig. 10(a)). A lower release of fission gas in the APZ fuel is correlated with higher

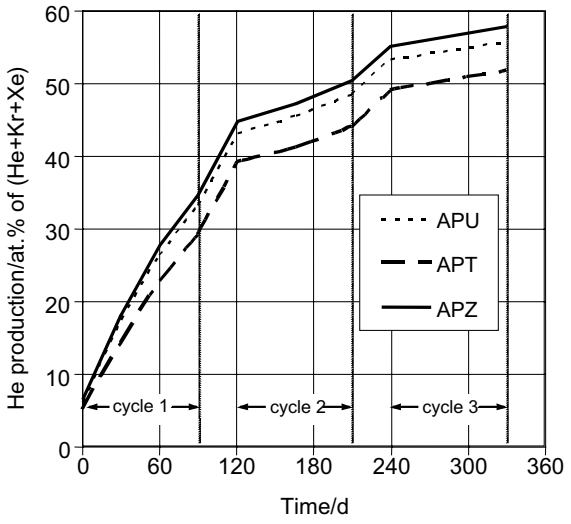

Fig. 8. Evolution of the relative of helium in the noble gas produced in the peak pellets of the studied fuels: APU = $(Am_{0.25}Pu_{0.25}U_{0.5})O_{2-x}$; APT = $(Am_{0.25}Pu_{0.25}Th_{0.5})O_{2-x}$; APZ = $(Am_{0.25}Y_{0.1}Pu_{0.25}Zr_{0.4})O_{2-x}$.

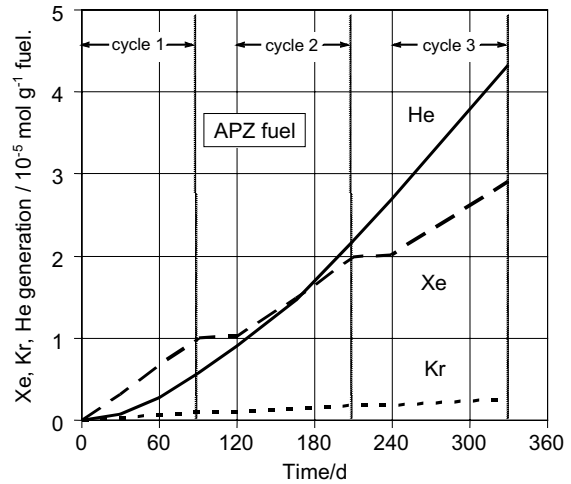

Fig. 9. Production of helium, xenon and krypton in the peak pellet of the APZ = $(Am_{0.25}Y_{0.1}Pu_{0.25}Zr_{0.4})O_{2-x}$ fuel over three cycles of radiation.

swelling and could be attributed to the formation of micro-bubbles. However, this hypothesis requires a more detailed analysis.

The release of helium starts in all three fuels at the beginning of the second cycle and shows very similar behaviour which can be attributed to the dominant role of the irradiation induced diffusion of He atoms. At the beginning of the second cycle the fraction of helium in the produced noble gas atoms is more than 40–45%, and

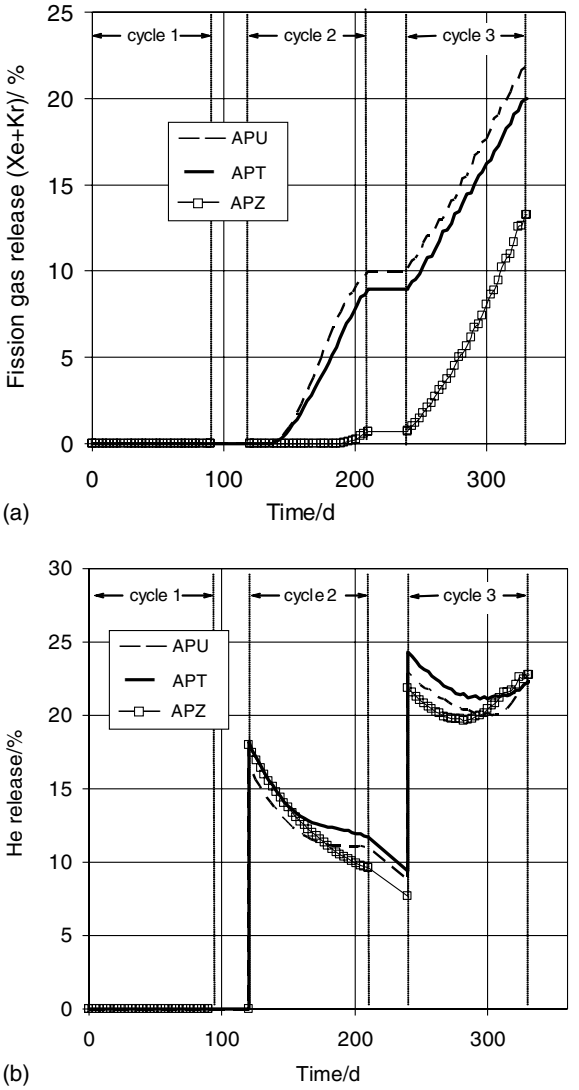

Fig. 10. Fractional release of xenon, krypton (a) and helium (b) in the studied fuels: APU = $(Am_{0.25}Pu_{0.25}U_{0.5})O_{2-x}$; APT = $(Am_{0.25}Pu_{0.25}Th_{0.5})O_{2-x}$; APZ = $(Am_{0.25}Y_{0.1}Pu_{0.25}Zr_{0.4})O_{2-x}$.

the traps of helium are almost saturated. A rapid temperature increase at the second cycle startup initiates a peak release of helium accumulated during the 'cold' maintenance period following the first irradiation cycle. Then the release rate decreases progressively over the cycle. The similar behaviour is also observed at the beginning of the third cycle. But here a minimum is observed in the He release – after the initial decrease, it begins to rise because the saturated traps cannot keep the newly generated helium. At the end of the third cycle, about 23% of the produced helium is released in all three samples (Fig. 10(b)).

The pressure in the fuel rods increases during the irradiation period from about 1 MPa (hot conditions) to 2.2–2.5 MPa which is significantly below the allowed limit of the cladding resistance. About half of the pressure increase can be attributed to the released helium.

Based on the obtained results of modelling one can conclude that longer irradiation experiments (at least for 2–3 cycles) may be performed with the proposed design of the target-fuel rods in the fast spectrum experimental channels of the MYRRHA subcritical core. It should be mentioned, however, that these results should be used with caution, as first approach, because the reliable experimental data for the properties of the considered actinide oxides mixtures are still missing and large uncertainty exists in the used input data. Approximation of the homogeneous ideal mixtures was used to estimate the fuel properties, and high temperature restructuring has not been taken into account yet. Development of more advanced models and code validation is under way.

6. Conclusions

The preliminary modelling of the behaviour of the fuel-target rods, containing americium–plutonium oxide fuel with different matrices (urania, thoria and yttria stabilised zirconia), were performed under typical irradiation conditions of the research ADS MYRRHA designed at SCK•CEN. The new fuel performance code MACROS, which has recently been developed, was used for calculations.

The first obtained results reveal that representative experiments on the americium burning in the $Am_{0.25}Pu_{0.25}U_{0.5}O_{2-x}$, $Am_{0.25}Pu_{0.25}Th_{0.5}O_{2-x}$, $Am_{0.25}Y_{0.1}Pu_{0.25}Zr_{0.4}O_{2-x}$ fuels can be performed in the MYRRHA subcritical core. The results of modelling demonstrate that neither fuel melting, nor cladding rapture can be expected after irradiation time of 270 EFPD and suggest that longer irradiation periods can be considered.

It was also shown that helium production in the considered fuels can affect fuel behaviour and contribute significantly in the internal pressure build-up, especially if the fuel rods have been stored for a long time before being re-irradiated. This effect has to be taken into account in all estimations concerning the TRU containing fuels.

The experimental data needed for validation of the used models and mixed oxide fuels properties are still very scarce therefore a large uncertainty exists in the obtained results of modelling. The validation of the MACROS code with recently published and new experimental data on the properties of actinide oxides and their compounds and on their behaviour under irradiation is therefore the primary objective of the following studies. In parallel, the modelling will be extended to include the longer irradiation times and other fuel compositions.

Acknowledgements

This work was supported by funds of the MYRRHA project of SCK•CEN and by funds of the FUTURE project of the EURATOM 5th Framework Programme.

References

[1] OECD/NEA Report 3109, OECD, 2002, Paris, France.
[2] H. Aït Abderrahim, P. Kupschus, E. Malambu, Th. Aoust, Ph. Benoit, V. Sobolev, K. Van Tiechelen, B. Arien, F. Vermeersh, Y. Jongen, D. Vandeplassche, in: Proceedings of 4th Meeting on Accelerator Driven Transmutation Technology and Applications (ADTTA'01), Reno, Nevada, USA, 11–15 November 2001.
[3] R.N. Hill, D.C. Wade, J.R. Liaw, E.K. Fujita, Nucl. Sci. Eng. 121 (1995) 17.
[4] Ch. De Raedt, B. Verboomen, Th. Aoust, H. Aït Abderrahim, E. Malambu, L.H. Baetsle, in: Proceedings of Second Workshop on Advanced Reactors with Innovative Fuels (ARWIF-2001), Chester, UK, 22–24 October 2001.
[5] W.S. Yang, Ann. Nucl. Energy 29 (2002) 509.
[6] S. Lemehov, P. Van Uffelen, V. Sobolev, in: Proceedings on The Enlarged Halden Programme Meeting, Storefjell, Norway, 2–6 September 2002, in press.
[7] S.E. Lemehov, M. SuzukI, J. Nakamura, Nucl. Technol. 3 (2001) 153.
[8] S.E. Lemehov, ANS Topical Meeting on LWR Fuel Performance, West Palm Beach, USA, 17–21 April 1994.
[9] S. Waters (Ed.), MCNPX User's Manual, Version 2.3.0., National Laboratory Report LA-UR-02-2607, April 2002.
[10] ORIGEN 2.1: Isotope generation and depletion code, Matrix exponential method, Oak Ridge National Laboratory, Oak Ridge, Tenessee, CC-371, August 1996.
[11] J. Belle, R.M. Berman, Report USDOE, DOE/NE-0060, 1984.
[12] E.P. Loewen, P.E. Mac Donald, J. Hohorst, in: Proceedings of the International Topic Meeting on Light–Water–Reactor–Fuel–Performance, Park City, Utah, USA, April 2000.
[13] C. Degueldre, U. Kasemeyer, F. Botta, G. Ledergerber, Mater. Res. Sci. Proc. 412 (1996) 15.
[14] R. Chawla, R.J.M. Konings, Prog. Nucl. Energy 38 (2001) 455.
[15] Project FUTURE, FP5 Programme Acronym: FP5-EA-ECTP C. Reference FIKW-CT-2001-00148, FP5 Project Record on the EC website: http://dbs.cordis.lu.
[16] M. Eriksson, J. Wallenius, J.E. Cahalan, K. Tucek, W. Gudowski, in: Proceedings of 3rd International Workshop on Utilisation and Reliability of High Energy Proton Accelerators, Santa Fe, New Mexico, USA, 12–17 May 2002.
[17] Chart Nuclides. Knolls Atomic Power Lab., Naval Reactors, US DOE, 15th Ed., 1996.

[18] OECD/CSNI/PWG2 Task Force on Fuel Safety Criteria, Fuel safety criteria technical review, OECD/NEA Report NEA/CSNI/R (99) 25, July 2000.
[19] H. Bailly, D. Menessier, C. Prunier (Eds.), Le combustible nucléaire des réacteurs à eau sous pression et des réacteurs à neutrons rapides, Collect. du CEA, Eyrolles, Paris, 1996.
[20] C. Ronchi, J.P. Ottaviani, C. Degueldre, R. Calabrese, in: European Research on Materials for Transmutation II, Karlsruhe, Germany, 26–27 September J. Nucl. Mater. (2003). doi:10.1016/S0022-3115(03)00171-5.
[21] A. Mignanelli, R. Thetford, in: The Second Workshop Proceedings on Advanced Reactors with Innovative Fuels (ARWIF-2001), Chester, UK, 22–24 October 2001.
[22] H. Blank, R. Linder (Eds.), Plutonium 1975 and Other Actinides, North-Holland, Amsterdam, 1976.
[23] C. Brown, V. Levy, J.L. Seran, K. Ehrlich, R. Roger, H. Bergmann, in: Proceedings of Interneational Conference on Fast Reactors and Related Fuel Cycles, Kyoto, Japan, 28 October–1 November 1991.
[24] F. Barbier, G. Benamati, C. Fazio, A. Rusanov, J. Nucl. Mater. 295 (2001) 149.
[25] M. Suzuki, Japan Atomic Energy Research Institute Report JAERI-DATA/CODE-2000-030, Japan, 2000.
[26] C. Kittel, Introduction to Solid State Physics, Wiley, 1976.
[27] H. Serizawa, Y. Arai, J. Alloys Comp. 312 (2000) 257.
[28] T. Yamashita, N. Nitani, T. Tsuji, J. Nucl. Mater. 245 (1997) 72.
[29] J. Callaway, Phys. Rev. 113 (1959) 1046.
[30] S. Lemehov, P. Van Uffelen, V. Sobolev, Paper F5.7, in: Proceedings of the Enlarged Halden Reactor Programme Meeting, Storefjell, Norwary, 2–6 September 2002, in press.
[31] Lemehov, P. Van Uffelen, V. Sobolev, in: Proceedings of 2nd European. Seminar on Materials for Transmutation (ERMT-II), ITU-FZK, Karlsruhe, Germany, 26–27 September 2002, J. Nucl. Mater. (2003). doi:10.1016/S0022-3115(03)00172-7.
[32] M. Ziman, Electroms and Phonons. The Theory of Transport Phenomena in Solids, Oxford classic series, Clarendon Press, Oxford, UK, 2001.
[33] J.P. Pirot, M. Pelletier, J. Pavageau, in: Seminar Proceedings on Fission Gas Behaviour in Water Reactor Fuels, CEA, Cadarache, France, 26–29 September 2000.
[34] J.-Fr. Babelot, N. Chauvin, Joint CEA/ITU Synthesis Report of the Experiment SUPERFACT-1, Technical Note JRC-ITU-TN-99/03, 1999.
[35] P. Van Uffelen, PhD Thesis, University of Liège, January 2002.
[36] P.M.G. Damen, Hj. Matzke, C. Ronchi, J.-P. Hiernaut, T. Wiss, R. Fromknecht, A. van Veen, F. Labohm, Nucl. Instrum. and Meth. B 191 (2002) 571.
[37] T. Wiss, J.-P. Hiernaut, J.R.M. Konings, C.T. Walker, P. Damen, R.P.C. Scharm, K. Baker, F.C. Klassen, R. Conrad, in: Proceedings of 2nd Seminar on European Research on Materials for Transmutation (ERMT-II), Karlsruhe, Germany, 26–27 September 2002, in press.
[38] A. van Veen, in: Proceedings of 2nd Seminar on European Research on Materials for Transmutation (ERMT-II), Karlsruhe, Germany, 26–27 September 2002, in press.
[39] R.P.C. Scharm, K. Baker, F.C. Klassen, E.A.C. Neef, R. Conrad, in: Proceedings of 2nd Seminar on European Research on Materials for Transmutation (ERMT-II), Karlsruhe, Germany, 26–27 September 2002, in press.